Journal of Al-Azhar University Engineering Sector

Vol.16, No. 61, October, 2021, 1111-1121

EFFECT OF NANO SIC PARTICLES ON THE CHARACTERIZATION OF SIC/CU NANO-COMPOSITE

M.A. Metwally[1], M. M. Sadawy[2], M. Ghanem[3], I. G. El-Batanony[4]

[1]Egyptian Natural Gas Company (GASCO), Cairo, Egypt.

[2]Mining and Pet. Dept., Faculty of Engineering, Al-Azhar University, Nasr City, Cairo, Egypt.

[3]Industrial Education, Suez University, Suez, Egypt.

[4] Mech. Eng. Dept. Faculty of Engineering, Al-Azhar University, Nasr City, Cairo, Egypt.

*Corresponding Author E-mail: mtayea00@gmail.com

ABSTRACT

In the present investigation, the influence of nano-SiC on characterization of SiC/Cu nano-composite was investigated. Electron microscope (SEM) was used for microstructure and morphology examinations. The erosion properties were investigated using pin on disc technique in oil environment. The results indicated that the grain structure of the copper matrix was reduced with increasing SiC nano-particles. The erosion resistance increased by increasing nano-SiC content to 5, 10, 15 and 20 (vol. %) respectively. Furthermore, the study was also extended to examine the influence of SiC content on the nuclear properties using winXCom computer program (version 3.1). It was found that there is no a significant variation in nuclear properties of Cu when the SiC is incorporated into the matrix at al l percentages.

KEYWORDS: Powder metallurgy; Composites; Erosion; Fusion reactors.

دراسة تأثير دقائق السيليكون كربيد متناهية الصغر علي خصائص متراكبة السيليكون كربيد /نحاس

محمود متولي[١] , مسعد محمد[٢] , محمد غانم[٣] , اسماعيل غازي[٢]

[١]شركة جاسكو مصر للغاز الطبيعي

[٢] كلية الهندسة جامعة الأزهر,

[٣] جامعة قناة السويس للتعليم الصناعي

الملخص

في هذا البحث تم دراسة تأثير دقائق السيليكون كربيد متناهية الصغر علي خصائص متراكبة السيليكون كربيد /نحاس . وقد استخدت عدة اجهزة متنوعة منها الماسح الالكتروني كما استخدم برنامج اكس كوم لعمل دراسة نووية علي تلك المتراكبات بنسب اضافة مختلفة وقد بينت النتلئج ان اضافة دقائق السيليكون كربيد متناهية الصغر قد ادى الى تحسن في خصائص تلك المتراكبة .

1. INTRODUCTION

Copper-based alloys in magnetic containment thermonuclear fusion reactors have been considered as candidate materials for the first wall and stabilizers for superconducting coils [1-3]. In reactor designs that feature high thermal loads on the first wall, their use as a first wall material has been suggested. For highly-loaded divertor collector plates, other designs use copper as a heat sink, in conjunction with other materials. Compared to traditional alloys big value of copper-based alloys [4]. Further many authors reported that copper is an ideal container material because of its thermal stability under the anaerobic conditions [5]. The development of heat sink materials with high thermal conductivity and sufficient strength under the service loading is required for the efficiency of future fusion reactors [6]. Improving the mechanical properties has been a major goal in recent years for the copper alloys. A very favorable class of copper alloys for the above applications is incorporating hard particles into copper matrix. Incorporating hard particles into metal matrix block the movement of dislocation which has a pronounced strengthening effect [6]. Aghamiri et al. [7] found that incorporating Y_2O_3 Nano sized into copper matrix improved the mechanical properties of copper to be used in fusion material application. It is known that the hard particles ceramic materials can be incorporated into the metal matrix using casting and powder techniques. However, few new techniques such as electroforming and thermal spraying have also been used to fabricate Cu composites [8]. The powder route can be considered as the most economical rout due to providing uniform distribution of reinforcement particles into the matrix without agglomeration problems. [9]. Among the reinforcements used in fabrication of metal matrix composites, SiC particles are a potential reinforcement for Cu owing to their unique properties such as excellent resistance to oxidation and corrosion, high hardness, low coefficient of thermal expansion and low cost [5]. Yunlong et al. [10] investigated the effect of SiC on the properties of Cu matrix containing different SiC content. The results found that the thermal expansion coefficient and the wear resistance of the composites decreased with growing SiC content. Compared with the pure Cu matrix, the obtained composites have better wear resistance. Additionally Efe et al. [11] found that incorporating SiC in copper matrix reduces the electrical conductivity of the matrix. In our previous work [9,12], the obtained results showed that the corrosion resistance of copper increased significantly with increment of SiC content due to improvement in patina passive film.

In this investigation the influence of SiC content on the mechanical and abrasion behavior of Cu composite in oil environments was studied. The study was also extended to examine the influence of SiC content on the nuclear properties using winXCom computer program (version 3.1).

2. MATERIAL AND METHODS

2.1 Material

Cu and SiC nano powders with average particle size of 70 and 50 nano respectively were used in this study. The different xSiC/Cu nano-composites were fabricated by powder metallurgy technique whereas, (x=5, 10, 15 and 20 vol. %). The powders were mixed together using a mixer with 10 cm diameter and speed of 950 rpm for 3 h for obtaining composites with uniform distribution. The powders were cold compacted using universal testing machine at constant pressure of 450 MPa on a disc steel die having a diameter with 12 mm and a thickness of 10 mm. The green compacted samples were sintered in electric tube furnace at 850 ^{o}C in presence of argon gas for 2 h. more details on the properties of material and fabrication can be found in [9,12].

2.2. Hardness

The hardness of the investigated materials was measured using Vicker hardness tester at load of 5 kg. The average value of 10 indentations was reported for each sample.

2.3. Abrasion Testing

All the abrasion tests were performed in oil environment using a pin-on-disc machine Fig.1 at speed of 0.25 m/s, applied load of 15, abrasive particles of 13μm and time of 30 min. The specimen was in contact with the rotating disc having a diameter of 140 mm. The normal load was applied on the specimen through a cantilever. After each test the specimens were dried, cleaned with a soft brush and weighed. The abrasion rates were calculated using Archard equation [١٢]:

$$\Delta V = K\frac{PL}{H} \qquad (١)$$

Where: V is the loss volume, L- wear distance, P- applied normal load, K -wear coefficient and H- hardness of material.

2.4 Gamma Mass Attenuation Coefficients

The mass attenuation coefficients (σ_{Th}) data of gamma rays was performed using WinXCom computer program software (Version 3.1) according to Eq. (4) [١٣] :

$$\sigma_{Th} = \sum_i^n W_i \left(\frac{\mu_i}{\rho_i}\right)_m \qquad (2)$$

The Half Value Layer (HVL, cm) is a significant factor in the assessment of the material's shielding efficiency in relation to its thickness per unit. The thickness that attenuates half of the radiation passing through the material refers to HVL. The HVL is derived from the formula below:

$$\text{Half value layer (HVL)} = \frac{\ln 2}{\mu} \qquad (3)$$

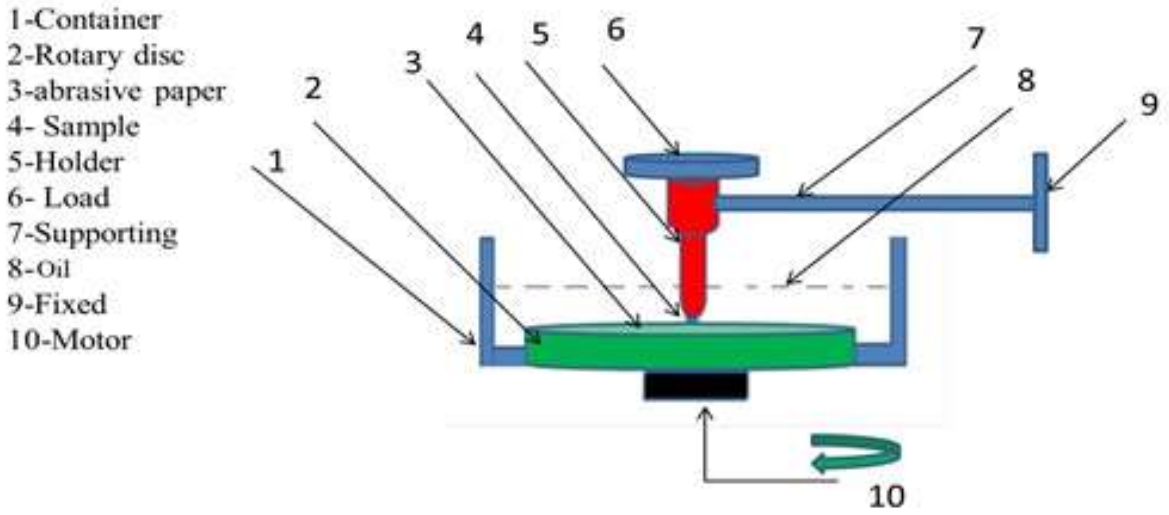

Fig. 1: A schematic sketch of wet pin on the disc

Similarly, the tenth value layer (TVL, cm) symbolizes the material thickness, which reduces the passing radiation by a factor of one-tenth of the initial amount. TVL can be calculated using the following equation:

$$\text{Tenth value layer (TVL)} = \frac{\ln 10}{\mu} \qquad (4)$$

The mean free path (MFP, cm), which is basically the average distance taken by moving particles between two consecutive collusions, is another factor influencing the efficiency of attenuation in radiation shielding. The MFP is calculated based on the following formula:

$$\text{Mean free path (MFP)} (\lambda) = \frac{\mathbf{1}}{\boldsymbol{\mu}} \qquad (5)$$

Mean free path $(\lambda) = \frac{1}{\mu}$: The mean free 'path is the average distance a gamma ray travels in the absorber before interacting;

Where: $(\lambda) = \frac{1}{\mu}$ is denotes to the mass attenuation coefficient of the actual element, while Wi is referring to the fractional weight of the element in each sample.

3. Results And Discussions

3.1. Microstructure

Figure 2 shows the SEM photographs of SiC/Cu composites with different SiC contents after sintering at 900 ºC. It clear that the SiC particles are homogeneously dispersed inside the matrix. Increasing the SiC content, the SiC particles move towards the grain boundaries, forming a homogenous network and uniformly dispersed inside the matrix as well. Furthermore, Fig. 2 shows that the grain size of Cu obviously is reduced with growing SiC content. This is due to the pinning effect of SiC that limits the grains growth of the matrix.

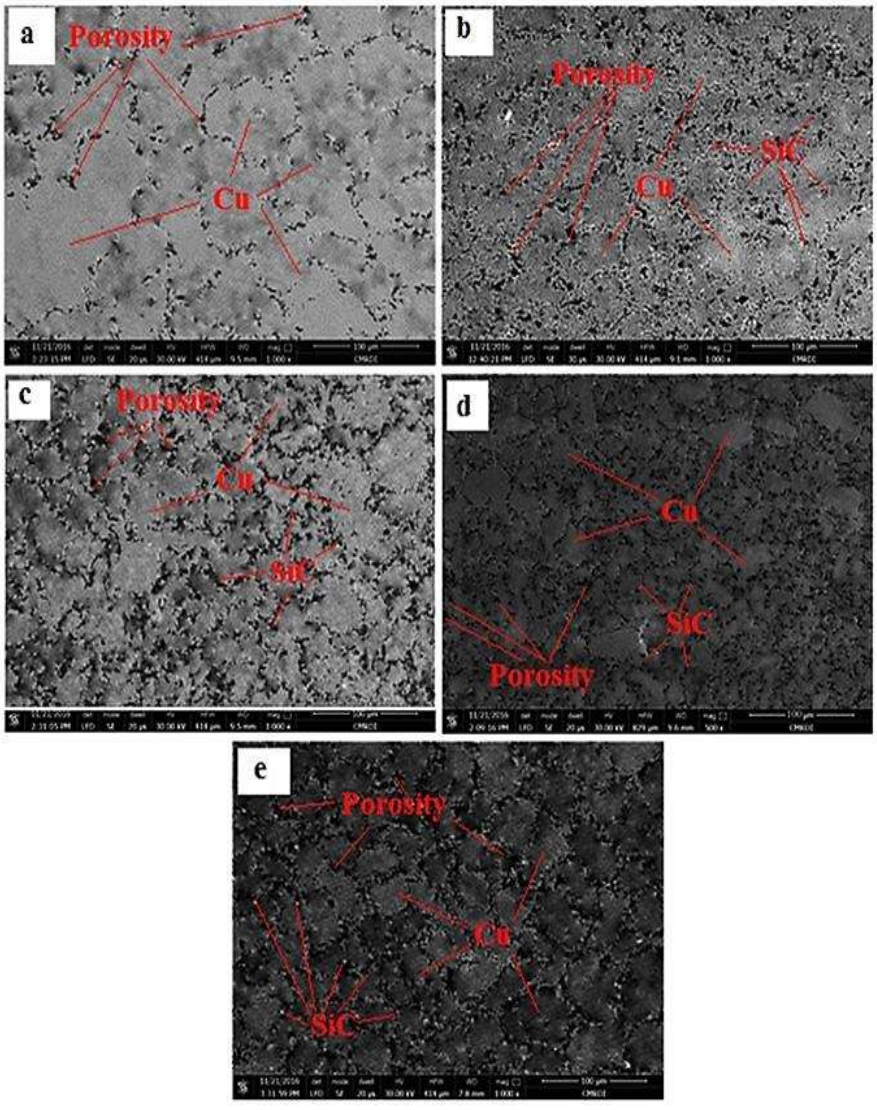

Fig.2: Microstructure of SiC/Cu nano-composites with different SiC contents sintered at 860 ºC. (a) 0.0 vol. % SiC, (b) 5 vol. % SiC, (c) 10 vol. % SiC, (d) 15vol. % SiC and (e) 20 vol. % SiC

3.2. Hardness Measurements

The hardness value of nano-Cu alloy with different values of nano-SiC content is shown in Fig.3. It is clear that all composite samples indicate higher hardness comparing to Cu sample. The hardness value increases by 28, 39, 65, and 77 % respectively; with an increment of nano-SiC content to 5, 10, 15, and 20 vol. %, respectively. This trend is due to the difference in the thermal contraction at the interface of SiC-Cu. This causes a strain field resulting in an increase in the dislocations. Increasing the dislocation reduces the plastic deformation of the composite.

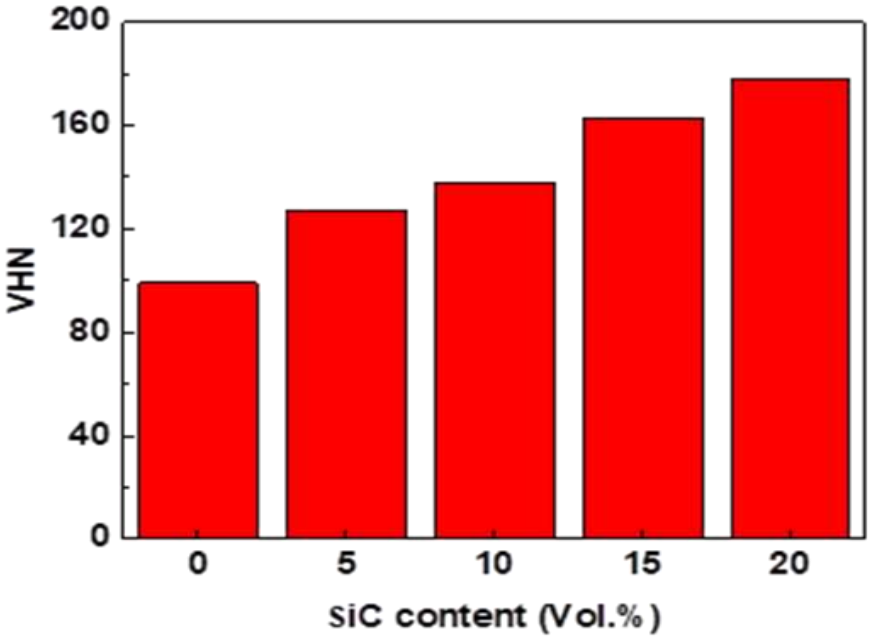

Fig.3: Effect of SiC content on the hardness of Cu/SiC nano composites

3.3. Effect Of Sic Content On The Abrasion Behavior Of Sic/Cu Composites In Oil Environment

The effect SiC content of the abrasion behavior SiC/Cu Nano composites in oil environment is shown in Fig. ٤. It is obvious that increasing SiC content from 5 to 20 (vol. %), the abrasion rate decreases for all percentages when compared with the base Cu. This enhancement in abrasion resistance is attributed to presence of hard SiC nano-particles in the Cu-matrix. These particles act as a load carrier and protect the Cu-matrix from damage. However, it is interesting to note that the gradient of decreasing in abrasion rate depends on the amount of SiC in the matrix. This is due to the worn surfaces of the investigated alloys are shown in Fig. ٥. Clearly the pure Cu alloy as shown in Fig 2a displays continuous parallel grooves. The behavior suggests that the dominant abrasion mechanism of pure Cu alloy belongs to the abrasive mechanism [١٤]. Further, Fig. 5a shows that the grooves are wider and deeper suggesting an augmented metallic contact Fig 5b shows that SiC/Cu composites with 5 SiC (vol %) suffers from plastic deformation and adhesive wear in several places. Increasing the SiC to 20 SiC (vol %), both the plastic deformation and adhesive wear decreased greatly. This behavior may be attributed to many reasons: firstly, a tribo film covers the entire surface and therefore, it decreases the adhesive wear. Secondly, the uniform distribution of SiC in the matrix. These two factors decrease the adhesive wear. Similar results were obtained in sea water environment for these samples in our previous work [12].

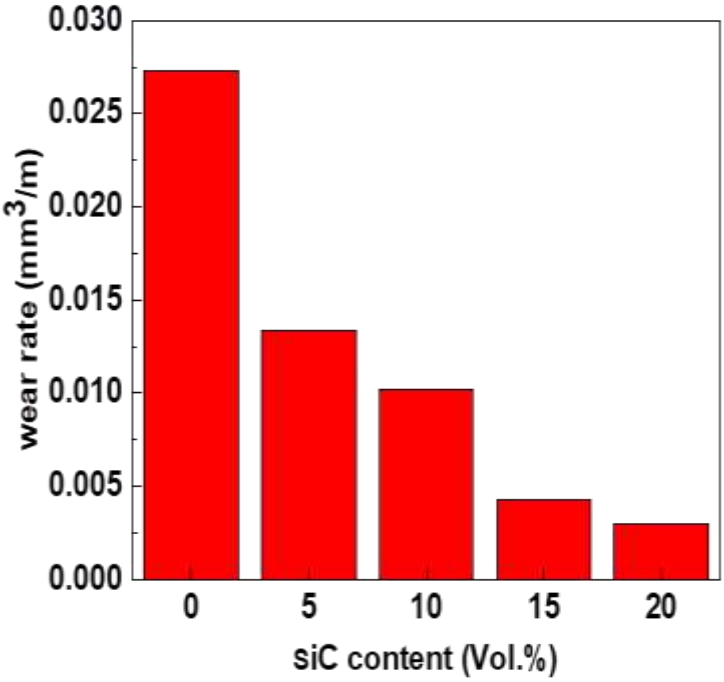

Fig.4: Effect of SiC content on the abrasion behavior of Cu/SiC nano composites

3.4. Effect Of Sic Content On The Nuclear Radiation Shielding Behavior Of Sic/Cu Composites

Data on the scattering and absorption of photons (x-rays and gamma rays) are required for many applications in science, engineering, and medicine. The win XCOM program has the ability to generate cross sections on standard energies.

This software provides total cross sections and attenuation coefficients as well as partial cross sections for the following processes: incoherent scattering, coherent scattering, photoelectric absorption, and pair production in the field of the atomic nucleus and in the field of the atomic electrons [1٤]. Therefore, the intensity distribution of gamma rays transmitted through SiC/Cu barriers of the investigated samples were calculated and plotted at different incident gamma-ray energy lines as shown in Fig. 6.

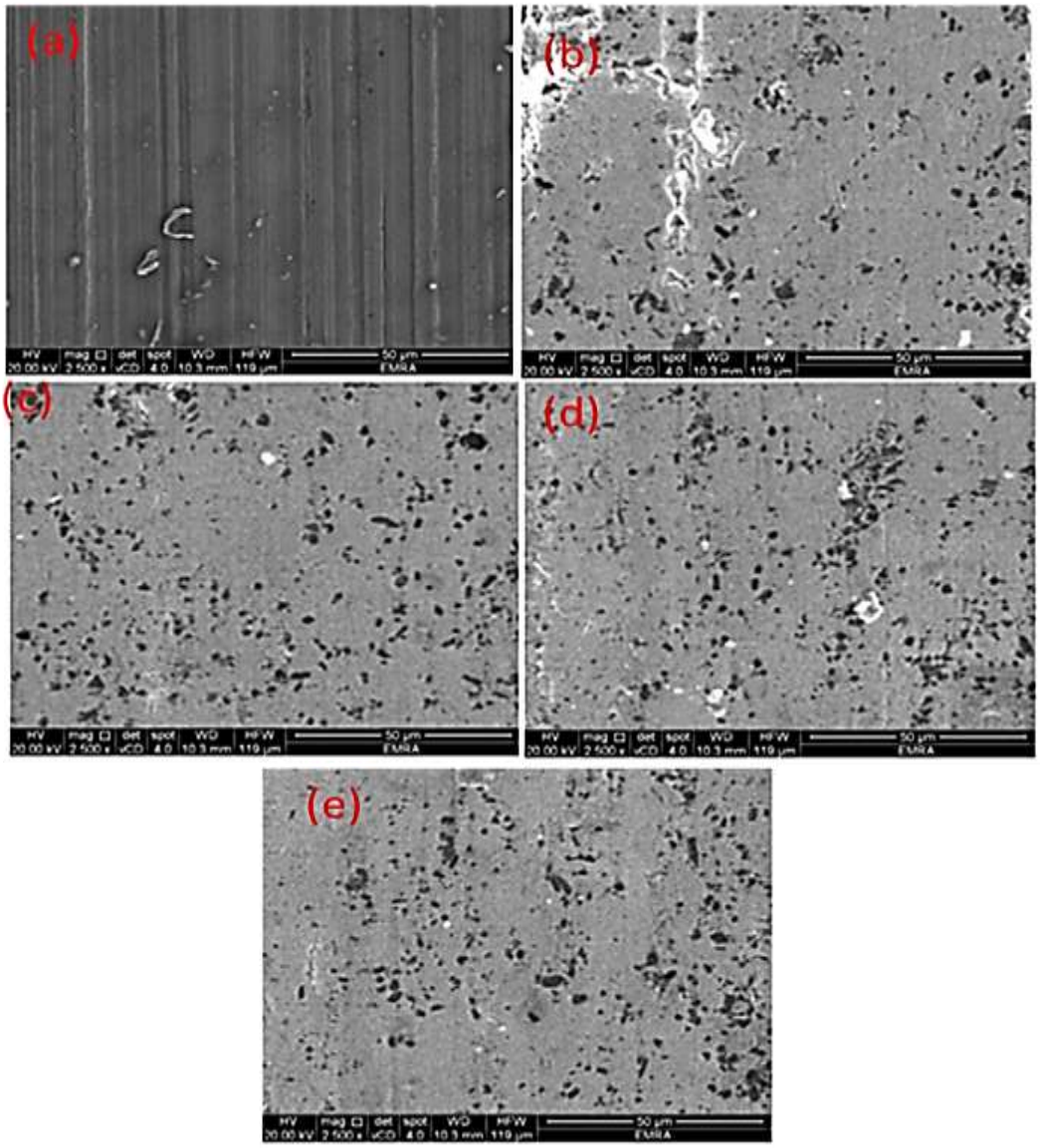

Fig.5: The worn surfaces of the investigated samples after abrasion in the oil

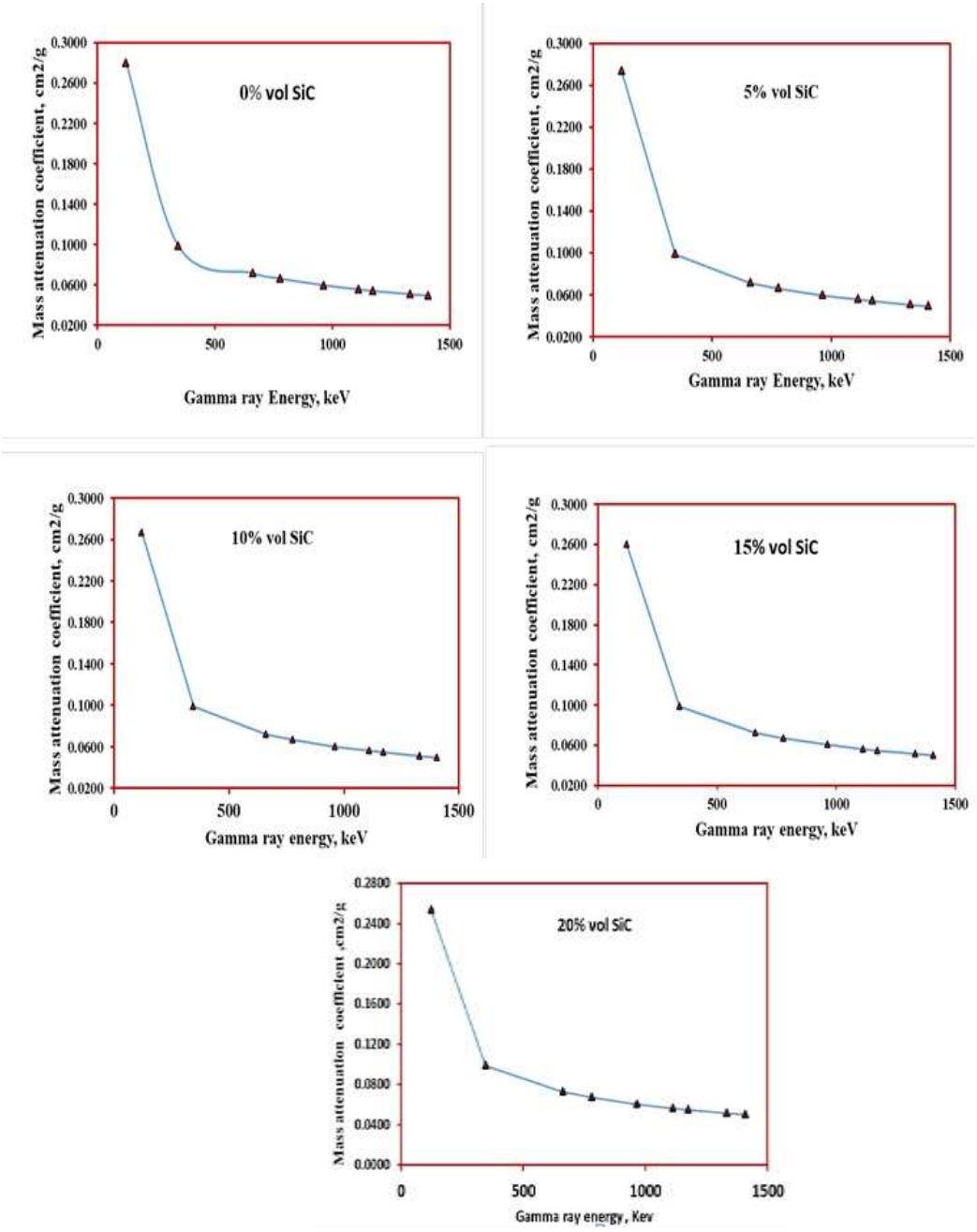

Fig. ٦: Mass attenuation coefficients of SiC/Cu samples as a function of gamma ray energy

Clearly, it can be seen that the behavior of all curves can be separated into two areas. The first area from (121 to 400) keV was ascribed by a sharp reduction in the values of mass attenuation coefficients (σ, cm2/g) with the growth of gamma-ray energies. The behavior is due to the photoelectric reaction which predominates among the examined alloy barriers and gamma rays [15]. The second region from (400 to 1407) keV defines by a slight decrease in the values of mass attenuation coefficients with the increment of gamma-ray energies. This is ascribed to the Compton scattering reaction which predominates in this stage [16]. Further, Fig. ٧ shows that the values of σ (by cm^2/g) did not change significantly by increasing the SiC content up to 1407 keV gamma ray energy. Generally, the values of mass attenuation coefficients directly depend on the density of material. However, in our case our samples still have approximately the same mass attenuation values. This behavior is a good result for many applications. The comparisons of half and tenth value layers of the investigated alloys at the gamma ray energy lines is shown in Tables 1-5 for all investigated samples. The value of mean free paths was also calculated and presented in Tables 1-5. The presented data shows that there is no significant variation in radiation properties of Cu when the SiC is incorporated into the matrix at all percentages.

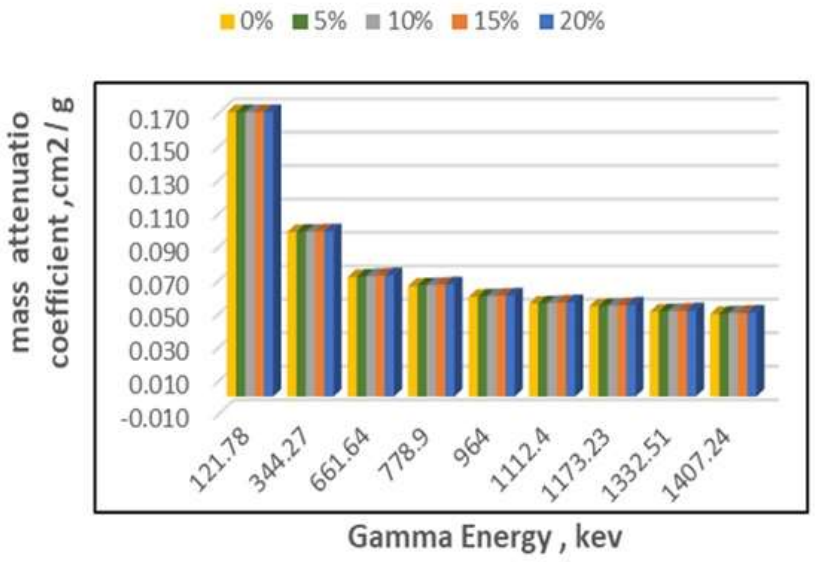

Fig.7: Comparison between mass attenuation coefficients of SiC/Cu samples with different gamma ray energies

Table 1: Attenuation properties of Cu

Energy, keV	Linear att. Co.	M att. Co. Ex.	HVL	Tvl	Mean free path (MEP)
121.78	2.351757362	0.2734	0.294758299	0.979055083	0.425213934
344.27	0.8468563	0.09845	0.81855682	2.718879225	1.180837883
661.64	0.61675568	0.0717	1.123945871	3.733244906	1.621387581
778.9	0.570735556	0.06635	1.214573006	4.034267668	1.752124937
964	0.514565199	0.05982	1.347156787	4.474651617	1.943388325
1112.4	0.478781327	0.05566	1.447842597	4.809084796	2.088636176
1173.23	0.466136545	0.05419	1.4871179	4.939539763	2.145294142
1332.51	0.437492244	0.05086	1.584485233	5.262950447	2.285754809
1407.24	0.425879689	0.04951	1.627689739	5.406456468	2.348080985

Table 2: Attenuation properties of 5 % vol SiC/Cu composite

Energy, keV	Linear att. Co.	M att. Co. Ex.	HVL	Tvl	Mean free path (MEP)
121.78	2.205818267	0.2667	0.314259797	1.043830325	0.453346504
344.27	0.815333951	0.09858	0.850203771	2.823996224	1.226491303
661.64	0.595331079	0.07198	1.164394106	3.86759583	1.679737602
778.9	0.550999674	0.06662	1.25807697	4.178768355	1.814883107
964	0.496908742	0.06008	1.395024763	4.6336476	2.012441954
1112.4	0.462336862	0.0559	1.499339673	4.980135023	2.162925092
1173.23	0.450178809	0.05443	1.539832588	5.114634353	2.221339567
1332.51	0.42247168	0.05108	1.640820042	5.450069456	2.367022565
1407.24	0.411223413	0.04972	1.685701684	5.599146175	2.431768154

Table 3: Attenuation properties of 10 % vol SiC/Cu composite

Energy, keV	Linear att. Co.	M att. Co. Ex.	HVL	Tvl	Mean free path (MEP)
121.78	2.065109983	0.2601	0.335672195	1.114952724	0.484235711
344.27	0.783725515	0.09871	0.884493342	2.937890826	1.275956928
661.64	0.573721059	0.07226	1.208252668	4.013274334	1.743007311
778.9	0.531084993	0.06689	1.305252471	4.335464246	1.882937783
964	0.479000712	0.06033	1.447179476	4.806882205	2.087679568
1112.4	0.445733466	0.05614	1.555189487	5.165643096	2.243493201
1173.23	0.433982744	0.05466	1.597298533	5.30551049	2.304239084
1332.51	0.407305429	0.0513	1.701916916	5.653005914	2.455160006
1407.24	0.396428072	0.04993	1.748614817	5.80811543	2.522525702

Table 4: Attenuation properties of 15% vol SiC/Cu composite

Energy, keV	Linear att. Co.	M att. Co. Ex.	HVL	Tvl	Mean free path (MEP
121.78	2.065109983	0.2601	0.335672195	1.114952724	0.484235711
344.27	0.783725515	0.09871	0.884493342	2.937890826	1.275956928
661.64	0.573721059	0.07226	1.208252668	4.013274334	1.743007311
778.9	0.531084993	0.06689	1.305252471	4.335464246	1.882937783
964	0.479000712	0.06033	1.447179476	4.806882205	2.087679568
1112.4	0.445733466	0.05614	1.555189487	5.165643096	2.243493201
1173.23	0.433982744	0.05466	1.597298533	5.30551049	2.304239084
1332.51	0.407305429	0.0513	1.701916916	5.653005914	2.455160006
1407.24	0.396428072	0.04993	1.748614817	5.80811543	2.522525702

Table 5: Attenuation properties of 15% vol SiC/Cu composite

Energy, keV	Linear att. Co.	M att. Co. Ex.	HVL	Tvl	Mean free path (MEP
121.78	2.065109983	0.2601	0.335672195	1.114952724	0.484235711
344.27	0.783725515	0.09871	0.884493342	2.937890826	1.275956928
661.64	0.573721059	0.07226	1.208252668	4.013274334	1.743007311
778.9	0.531084993	0.06689	1.305252471	4.335464246	1.882937783
964	0.479000712	0.06033	1.447179476	4.806882205	2.087679568
1112.4	0.445733466	0.05614	1.555189487	5.165643096	2.243493201
1173.23	0.433982744	0.05466	1.597298533	5.30551049	2.304239084
1332.51	0.407305429	0.0513	1.701916916	5.653005914	2.455160006
1407.24	0.396428072	0.04993	1.748614817	5.80811543	2.522525702

4.

CONCLUSIONS

The effect of SiC on the characterization of Cu was investigated. The following main observations were made from this study:

1) The grain structure of the copper matrix was reduced with increasing SiC nano-particles.

2) The erosion resistance of Cu in oil environment was improved by increasing nano-SiC content.
3) The dominant abrasion mechanism of pure Cu belongs to the abrasive mechanism while SiC/Cu composites with 5 SiC (vol %) suffers from plastic deformation and adhesive wear in several places. Increasing the SiC to 20 SiC (vol %), both the plastic deformation and adhesive wear decreased greatly.
4) Incorporation of SiC into Cu matrix did not change the nuclear properties of Cu.

REFERENCES

[1] Burkart, W.2005. Introductoin: Status report on fusion research, Nucl. Fusion. 45 (2005). https://doi.org/10.1088/0029-5515/45/10A/E01.

[2] El-Guebaly, L.A. 2010. Fifty years of magnetic fusion research (1958-2008): Brief historical overview and discussion of future trends, Energies. 3 (2010) 1067–1086. https://doi.org/10.3390/en30601067.

[3] Ghodke, S.R., Dutta, B.K., Durgaprasad, P. V. 2020. Analytical development and experimental verification of empirical correlations to determine mechanical properties of copper alloys using small punch test data, Fusion Eng. Des. 159 (2020) 111786. https://doi.org/10.1016/j.fusengdes.2020.111786.

[4] Butterworth, G.J., Forty, B.A. 1992. A survey of the properties of copper alloys for use as fusion reactor materials, J. Nucl. Mater. 189 (1992) 237–276.https://doi.org/10.1016/0022-3115(92)90381-T.

[5] Akbarpour,M.R., Najafi, M., Alipour S., Kim H.S. 2019. Hardness, wear and friction characteristics of nanostructured Cu-SiC nanocomposites fabricated by powder metallurgy route, Mater. Today Commun. 18 (2019) 25–31. https://doi.org/10.1016/j.mtcomm.2018.11.001.

[6] Huang, B., Hishinuma, Y., Noto, H., Kasada, R., Oono, N., Ukai, S., Muroga, T. 2018. In-situ fabrication of yttria dispersed copper alloys through MA-HIP process, Nucl. Mater. Energy. 16 (2018) 168–174. https://doi.org/10.1016/j.nme.2018.06.024.

[7] Aghamiri,S.M., Oono, N., Ukai, S., Kasada, R., Noto, H., Hishinuma, Y., Muroga, T.2018. Microstructure and mechanical properties of mechanically alloyed ODS copper alloy for fusion material application, Nucl. Mater. Energy. 15 (2018) 17–22. https://doi.org/10.1016/j.nme.2018.05.019.

[8] Shaik, M.A., Golla, B.R.2020. Two body abrasion wear behaviour of Cu–ZrB2 composites against SiC emery paper, Wear. 450–451 (2020) 203260. https://doi.org/10.1016/j.wear.2020.203260.

[9] Metwally, M.A., Sadawy, M.M., Ghanem, M. 2018. The Egyptian International Journal of Engineering Sciences and Technology, Effect of SiC (p) Content on the Corrosion Behavior of Nano SiC (p) / Cu Composites, 26 (2018) 22–28. https://doi: 10.21608/eijest.2018.97259

[10] Ming, H., Yunlong, Z., Lili, T., Lin, S., Jing, G., Peiling, D. 2015. Surface modifying of SiC particles and performance analysis of SiCp /Cu composites, Appl. Surf. Sci. 332 (2015) 720–725. https://doi.org/10.1016/j.apsusc.2015.01.130.

[11] Efe, G.C., Altinsoy, I., Yener, T., Ipek, M., Zeytin, S., Bindal, C. 2010. Characterization of cemented Cu matrix composites reinforced with SiC, Vacuum. 85 (2010) 643–647. https://doi.org/10.1016/j.vacuum.2010.09.009.

[12] M.A. Metwally, M.M. Sadawy, M. Ghanem, I.G.E.- Batanony, The Role of Nano-SiC on Microstructure and Tribo-logical Properties of SiC/Cu Nano-Composite, J. Eng. Res. Reports. 15 (2020) 35–44. https://doi.org/10.9734/jerr/2020/v15i417153.

[13] Sadawy, M.M., El Shazly, R.M. 2019. Nuclear radiation shielding effectiveness and corrosion behavior of some steel alloys for nuclear reactor systems, Def. Technol. 15 (2019) 621–628. https://doi.org/10.1016/j.dt.2019.04.001.

[14] Metwally, M., Fattah, H. A., Ghanem, M., Batanony, I. 2018. Effect of Sic Content on Dry Sliding Wear Behavior of Nanosized Sic(P)/Cu Composites, J. Al-Azhar Univ. Eng. Sect. 13 (2018) 1260–1267. https://doi.org/10.21608/auej.2018.18937.

[15] J. Berger, MJ; Hubbell, XCOM Photon Cross Sections, Nist. 87 (1987) 26.

[16] El Shazly, R.M., Sadawy, M.M. 2017. Effect of Slag as a Fine Aggregate on Mechanical , Corrosion , and Nuclear Attenuation Properties of Concrete, 5 (2017) 243–250.